Supporting Information

Fluoride-Free and Seed-Free Microwave-Assisted Hydrothermal Synthesis of Nanosized High-silica Beta Zeolites for Effective VOCs Adsorption

Zhe Ma[a], Hua Deng[b,c], Lin Li[d], Qiang Zhang[a,e], Guangrui Chen[a], Chang Sun[a], Hong He*[,b,c,f], Jihong Yu*[, a, e]

[a]State Key Laboratory of Inorganic Synthesis and Preparative Chemistry, College of Chemistry, Jilin University, 2699 Qianjin Street, Changchun 130012, P. R. China

[b]Center for Excellence in Regional Atmospheric Environment, Key Laboratory of Urban Pollutant Conversion, Institute of Urban Environment, Chinese Academy of Sciences, Xiamen 361021, China

[c]University of Chinese Academy of Sciences, Beijing 100049, China

[d]Electron Microscopy Center, Jilin University, 2699 Qianjin Street, Changchun 130012, P. R. China

[e]International Center of Future Science, Jilin University, 2699 Qianjin Street, Changchun 130012, P. R. China

[f]Research Center for Eco-Environmental Sciences, Chinese Academy of Sciences, Beijing, 100085, China

***Corresponding author**: Tel/Fax: (+86) 431-85168608;

Email address: jihong@jlu.edu.cn

honghe@rcees.ac.cn

Contents

Figure S14. SEM images of Beta zeolites with varied Si/Al ratios obtained via two-step hydrothermal crystallization: (a) Beta-14-60-HT, (b) Beta-72-70-HT, (c) Beta-123-140-HT, (d) Beta-265-190-HT.

Figure S15. TEM images of Beta zeolites with varied Si/Al ratios obtained via two-step hydrothermal crystallization: (a) Beta-14-60-HT, (b) Beta-72-70-HT, (c) Beta-123-140-HT, (d) Beta-265-190-HT.

Figure S16. Dynamic light scattering characterization of Beta zeolites with varied Si/Al ratios obtained via two-step hydrothermal crystallization: (a) Beta-14-60-HT, (b) Beta-72-70-HT, (c) Beta-123-140-HT, (d) Beta-265-190-HT.

Figure S17. N_2 adsorption/desorption isotherms of Beta zeolites with varied Si/Al ratios obtained via two-step hydrothermal crystallization.

Figure S18. EPR spectra of the initial reaction mixture upon low-temperature hydrothermal for 12–48 h.

Figure S19. (a, b, c) Low-magnification scanning electron microscopy (SEM) images, (d, e, f) high-magnification SEM images of pure-silica Beta zeolites synthesized using different methods: (a, d) Beta-∞-HF, (b, e) Beta-∞-SAC, (c, f) Beta-∞-DA.

Table S1. Molar compositions of the initial mixtures and crystallization conditions of Beta zeolites.

Table S2. Fast synthesis of Beta zeolites with different Si/Al ratios particles summered from references.

Table S3. Selected pure-silica Beta zeolites reported in the literature and their synthesis methods, Si/Al ratios, and particle size.

Table S4. Porosities of pure-silica Beta zeolites synthesized by traditional synthesis methods.

Table S5. Intensities and assignments obtained from the deconvolution of the ^{29}Si MAS NMR for three pure-silica Beta zeolites.

Table S6. Langmuir, Sips equation correlation parameters and fitting results for different Beta zeolites.

1. Experimental Sections

1.1 Chemicals and reagents

All chemicals and reagents were supplied by commercial suppliers and used without further purification: LUDOX AS-40 colloidal silica (SiO_2, 40 wt%, Sigma-Aldrich Reagent Company), sodium aluminate ($NaAlO_2$, Sinopharm Chemical Reagent Company), tetraethylammonium hydroxide (TEAOH, 35 wt%, Alfa Aesar Company), sodium hydroxide (NaOH, 98%, Tianjin Yongsheng Chemical Reagent Company), fumed silica (Xuzhou Tiancheng Chlor-alkali Company), L-lysine ($C_6H_{14}N_2O_2$, 98%, Sinopharm Chemical Reagent Company).

1.2 Synthesis of samples

1.2.1 Synthesis of nanosized Beta zeolites with varied Si/Al ratios. A mixture with a molar composition of 1.0 SiO_2: 0.55 TEAOH: (0.00125–0.05) Al_2O_3: (0.017–0.078) Na_2O: 0.2 L-lysine: 6 H_2O was set for the synthesis of nanosized Beta zeolites with varied Si/Al ratios. Detailed synthetic conditions are listed in Table S1. Typically, colloidal silica, TEAOH, and deionized water were mixed at room temperature under stirring, followed by the addition of $NaAlO_2$, NaOH, and L-lysine. The gel mixture was kept on stirring under an infrared lamp to evaporate the excess water for the desired H_2O/SiO_2 ratio and then transferred into a microwave oven for irradiation at 80–100 °C for 4 h under 400 W of microwave power. Subsequently, the obtained mixture was then transferred into a Teflon-lined stainless-steel autoclave for hydrothermal treatment at 140 ºC for 6–10 h. The as-synthesized solid products were centrifuged, washed with water and ethanol several times, and then dried at 80 ºC in the oven overnight, followed by calcination at 550 ºC for 6 h. The as-prepared samples are denoted as Beta-x-y-MW, where x and y indicate their actual Si/Al ratio and particle size, respectively. To obtain the H-type Beta, the samples were ion-exchanged three times in 1 M NH_4NO_3 solution at 80 ºC for 3 h, and then calcined at 500 ºC for 6 h.

1.2.2 Synthesis of nanosized pure-silica Beta zeolite. A mixture with a molar composition of 1.0 SiO_2: 0.55 TEAOH: 0.016 Na_2O: 0.2 L-lysine: 6 H_2O was set for the synthesis of nanosized pure-silica Beta zeolite. The synthesis procedure was exactly the same as above, except that the conditions of microwave irradiation and hydrothermal treatment were adjusted to 100 °C for 4 h and 160 ºC for 120 h, respectively. The product was obtained by centrifugation, washed with water, and dried at 80 ºC overnight. After calcination at 550 ºC for 6 h, the obtained sample is denoted as Beta-∞-180-MW.

1.2.3 Synthesis of large-sized Beta zeolites. A mixture with a molar composition of 1.0 SiO_2: 0.55 TEAOH: (0.00125–0.025) Al_2O_3: (0.017–0.047) Na_2O: 0.2 $_L$-lysine: 6 H_2O was set for the synthesis of conventional Beta zeolites. The preparation procedure of gel mixture was exactly the same as in step 1.2. The crystallization was conducted at 80 °C for 48 h and subsequently at 140 °C for 48 h. The as-prepared samples are denoted as Beta-m-n-HT, where m and n indicate their actual Si/Al ratio and particle size, respectively. Detailed synthetic conditions are listed in Table S1.

1.2.4 Synthesis of pure-silica Beta zeolite via fluoride-mediated hydrothermal synthesis. A mixture with a molar composition of 1.0 SiO_2: 0.40 TEAOH: 0.40 HF: 7.5 H_2O was set for the synthesis of pure-silica Beta zeolite. Typically, TEAOH and deionized water were mixed at room temperature, followed by the addition of fumed silica while stirring for 1 h. After fast addition of HF and stirring, the mixture was kept on stirring under an infrared lamp to evaporate the excess water for the desired H_2O/SiO_2 ratio. The obtained gel mixture was then transferred into a Teflon-lined stainless-steel autoclave for hydrothermal treatment at 150 °C for 7 d. The as-synthesized solid products were centrifuged, washed with water and ethanol several times, and then dried at 80 °C overnight, followed by calcination at 550 °C for 6 h. The obtained sample is denoted as Beta-∞-HF.

1.2.5 Synthesis of pure-silica Beta zeolite via steam-assisted conversion. A mixture with a molar composition of 1.0 SiO_2: 0.42 TEAOH: 0.07 NaOH: 2.0 H_2O was set for the synthesis of pure-silica Beta zeolite. Typically, TEAOH, NaOH and deionized water were mixed at room temperature, followed by the addition of fumed silica in three equal lots while stirring. After stirring for 1 h, the mixture was kept on stirring under an infrared lamp to evaporate the excess water for the desired H_2O/SiO_2 ratio. As the water evaporated, a powder mixture (dry gel) was formed. 1.0 g powder mixture was transferred into a Teflon liner, and 0.5 mL water was added into the bottom of the liner without contacting the powder mixture. The crystallization was conducted at 140 °C for 5 d. The as-synthesized solid products were centrifuged, washed with water and ethanol several times, and then dried at 80 °C in the oven overnight, followed by calcination at 550 °C for 6 h. The as-prepared samples are denoted as Beta-∞-SAC. The same ion exchange procedure was followed as for Beta-x-y-MW in step 1.2.1

1.2.6 Synthesis of pure-silica Beta zeolite via dealumination. The process of dealumination was referred to the procedures described in Ref.1. The commercial H-Beta (Si/Al = 12.5) was purchased from Alfa Aesar Co., Ltd. Firstly, the parent H-Beta

was refluxed in 6 M HNO_3 suspension (50 mL/g) at 90 ºC for 24 h. Then, the product was collected by centrifugation and washed repeatedly with deionized water. The as-prepared samples are denoted as Beta-∞-DA.

1.3 Characterizations

The crystallinity and phase purity of the as-prepared samples were studied by powder X-ray diffraction (PXRD) on a Rigaku D-Max 2550 diffractometer using Cu Kα irradiation (λ = 1.5418 Å). The crystal sizes and morphologies were measured by scanning electron microscopy (SEM) using a JSM-7800F electron microscope, and transmission electron microscopy (TEM) using a Tecnai G2 S-Twin F20 electron microscope. High-resolution TEM (HRTEM) was obtained using JEM-2100F field emission electron microscope. The Si/Al ratios were determined with inductively coupled plasma (ICP) analyses carried out on a Perkin-Elmer Optima 3300 DV ICP instrument. Nitrogen adsorption/desorption measurements were performed on a Micromeritics 2020 analyer at 77.35 K after the samples were degassed at 350 ºC under vacuum. Solid-state ^{29}Si NMR and ^{27}Al NMR experiments were determined on Bruker Avance Neo 600Mz WB spectrometer with BBO MAS probe operating at a magnetic field strength of 14.1 T. The temperature-programmed desorption of ammonia (NH_3-TPD) experiments were performed using a Micromeritics AutoChemII 2920 automated chemisorption analysis unit with a thermal conductivity detector (TCD) under helium flow. Dynamic light scattering (DLS) measurements were carried out by photon correlation spectroscopy employing a Nano ZS90 laser particle analyzer (Malvern Instruments) at 25 °C. The electron paramagnetic resonance (EPR) spectra were recorded on a JEOL JES-FA 200 EPR spectrometer. The detailed instrumental parameters were as follows: scanning frequency: 9.4 GHz; central field: 3370 G; scanning width: 90 G; scanning power: 5 mW; scanning temperature: 293 K.

DMPO trapping is shown in the following reaction:

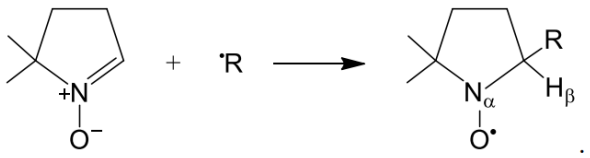

1.4 Performance test

Adsorption measurements of volatile organic compounds (VOCs).

In order to determine the adsorption equilibrium, static vapor-phase adsorption was performed using BELSORP-MAX. Each sample was degassed at 300 ºC for 3 h. The measurements were carried out at 30 ºC to construct the vapor adsorption isotherms.

Many models have been proposed to describe the isotherms, for example, Langmuir, Freundlich, Sips and Toth. In this study, the Langmuir and Sips equations were used to correlate the experimental data due to their explicit physical meanings.[2, 3] The Langmuir equation can be presented as follows:

$$q = \frac{q_m bp}{(1+bp)} \tag{1}$$

The Sips model is defined as follows:

$$q = \frac{q_m bp^{\frac{1}{n}}}{(1+bp^{\frac{1}{n}})} \tag{2}$$

where q is the adsorbed amount per unit weight of adsorbent (mmol g^{-1}), p is the relative pressure. q_m and b are common isotherm equation parameters for Langmuir and Sips. n is a specific parameter of the Sips model, which stands for the number of sites each sorbate molecule occupies.

In order to determine the dynamic adsorption behavior, breakthrough measurements were performed in a laboratory-built fixed-bed reactor (6 mm i.d.). A gaseous mixture of toluene (about 800 ppm) in N_2 balance at a mass flow of 100 mL min^{-1} was fed into the reactor under high relative humidity (RH=80%) at 30 ºC. A mixture of 0.1 g adsorbent and 0.3 g quartz sand was packed in the bed. Prior to all adsorption measurements, samples were pretreated at 300 ºC for 3 h. The concentrations of toluene were analyzed online by a gas chromatograph (Kefen, GC-9160, SE-54 capillary column) with a flame ionization detector. To confirm the measurement of dynamic adsorption, temperature-programmed desorption (TPD) measurements were carried out after the breakthrough measurements. Once the samples were saturated by the VOC flow, the feed gas was changed to pure nitrogen to purge for 0.5 h, followed by temperature ramping to 400 °C at a linear rate of 2 °C min^{-1}. The product was monitored by the same GC instrument.

2. Supplementary Figures and Table

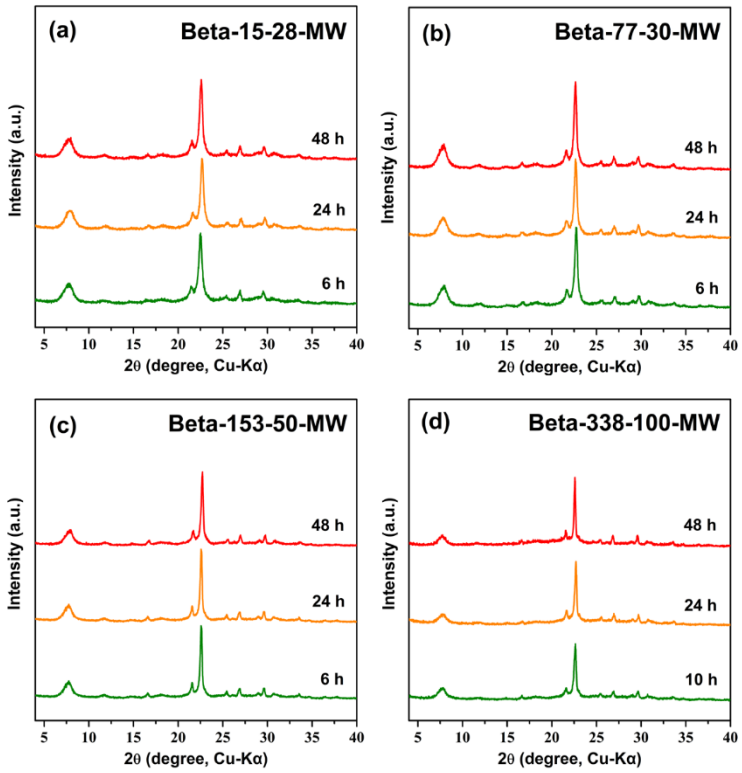

Figure S1. PXRD patterns of nanosized Beta zeolites with varied Si/Al ratios crystallized at 140°C for different periods.

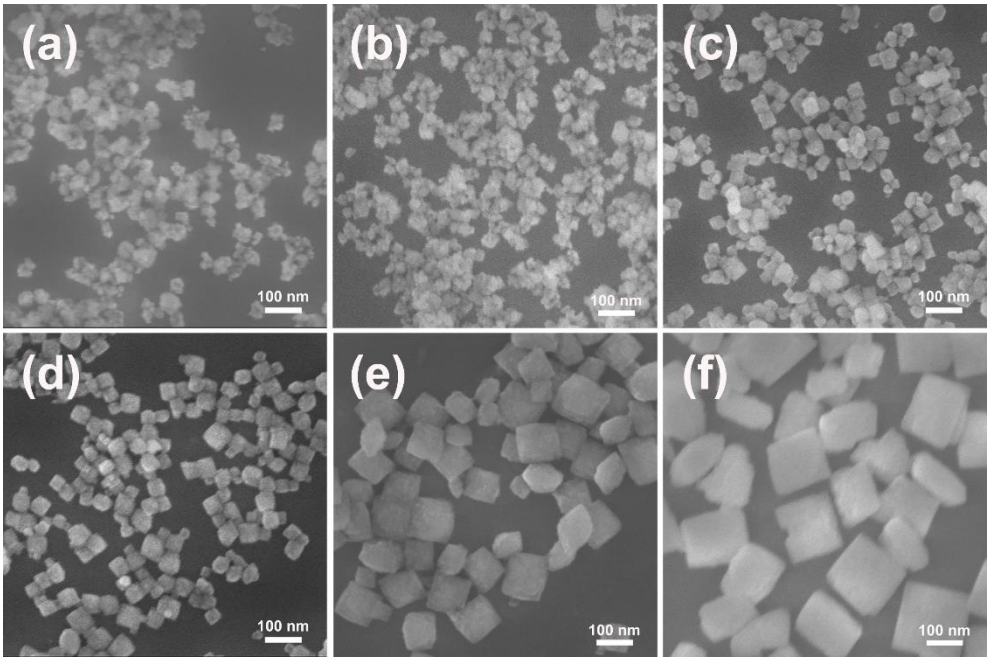

Figure S2. SEM images of nanosized Beta zeolites with varied Si/Al ratios: (a) Beta-9-25-MW, (b) Beta-15-28-MW, (c) Beta-77-30-MW, (d) Beta-153-50-MW, (e) Beta-338-100-MW, (f) Beta-∞-180-MW.

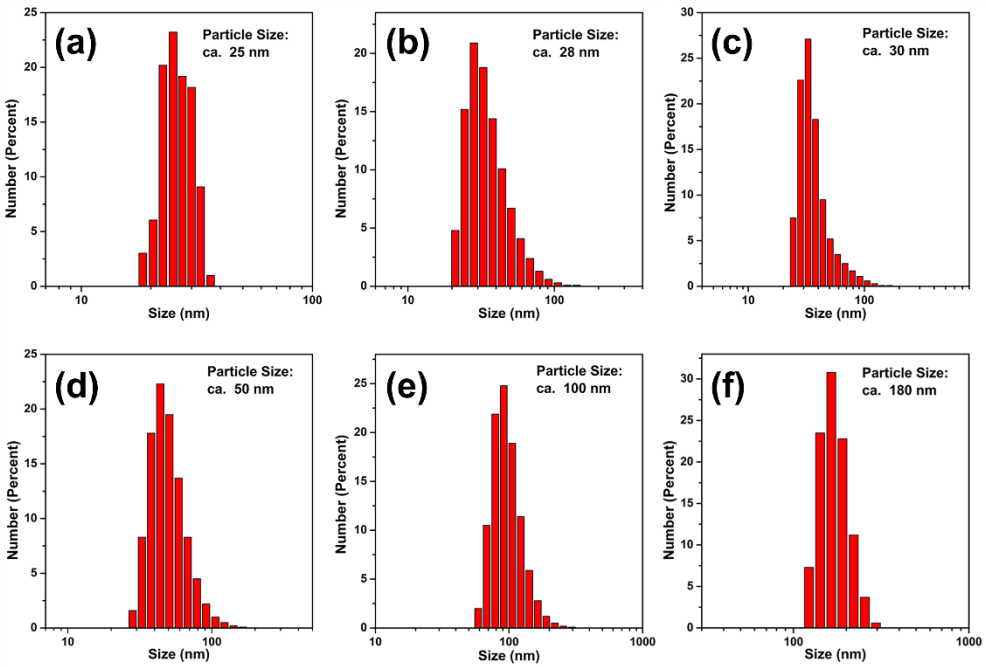

Figure S3. Dynamic light scattering characterization of nanosized Beta zeolites with varied Si/Al ratios: (a) Beta-9-25-MW, (b) Beta-15-28-MW, (c) Beta-77-30-MW, (d) Beta-153-50-MW, (e) Beta-338-100-MW, (f) Beta-∞-180-MW.

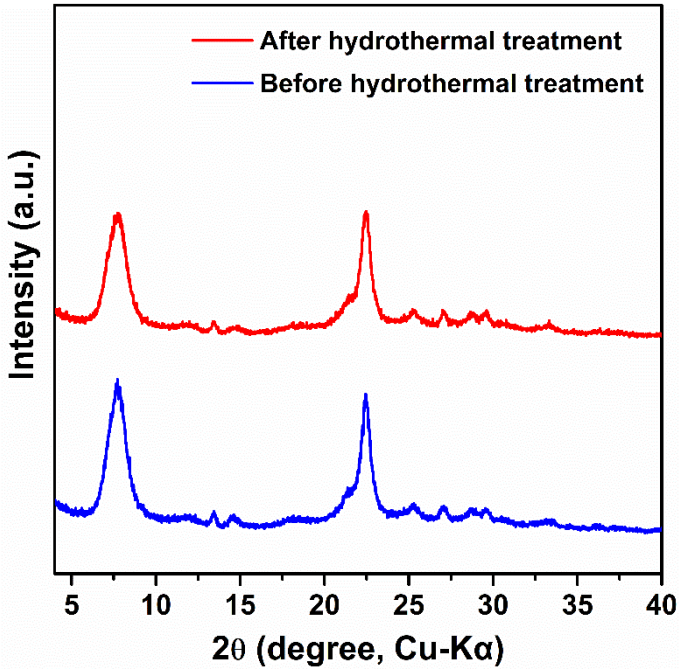

Figure S4. PXRD patterns of Beta-153-50-MW before and after 10% steam treatment at 750 °C for 3 h.

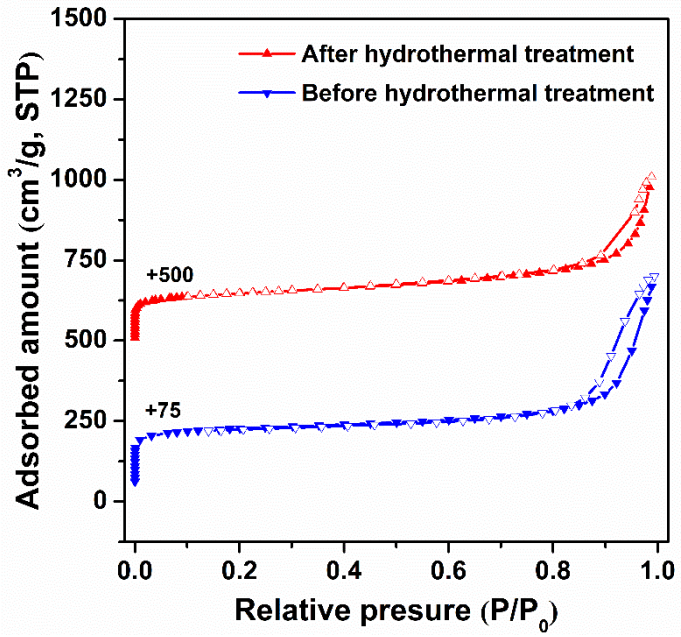

Figure S5. N_2 adsorption/desorption isotherms of Beta-153-50-MW before and after 10% steam treatment at 750 °C for 3 h.

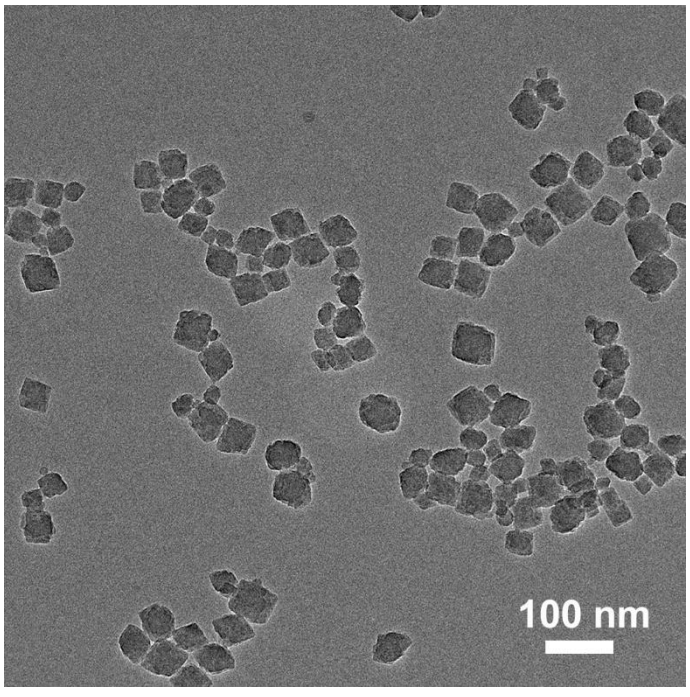

Figure S6. TEM image of Beta-153-50-MW after 10% steam treatment at 750 °C for 3 h.

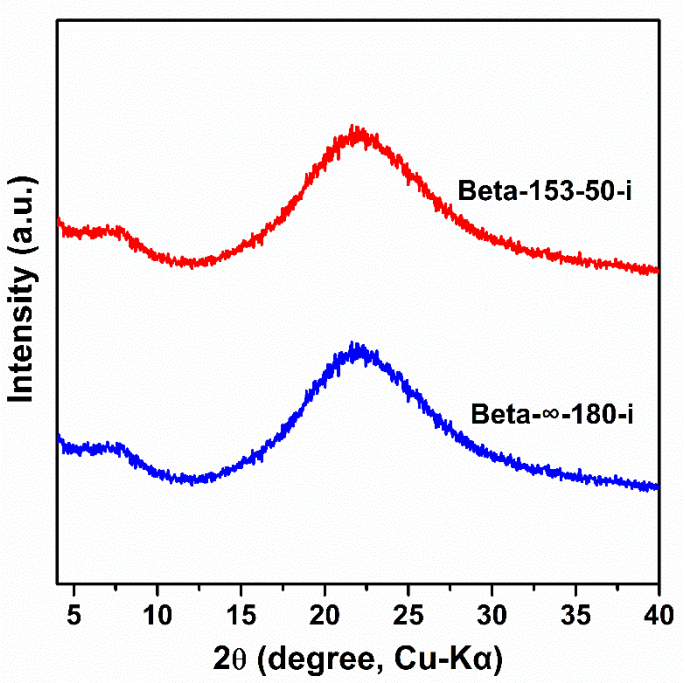

Figure S7. PXRD patterns of Beta-153-50-i and Beta-∞-180-i precursors treated after microwave synthesis.

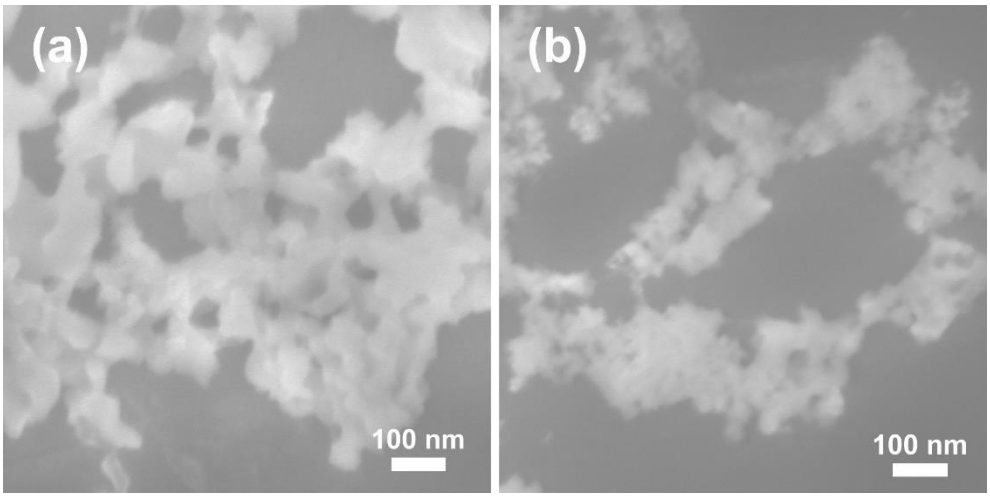

Figure S8. SEM images of precursors treated after microwave irradiation: (a) Beta-153-50-i, (b) Beta-∞-180-i.

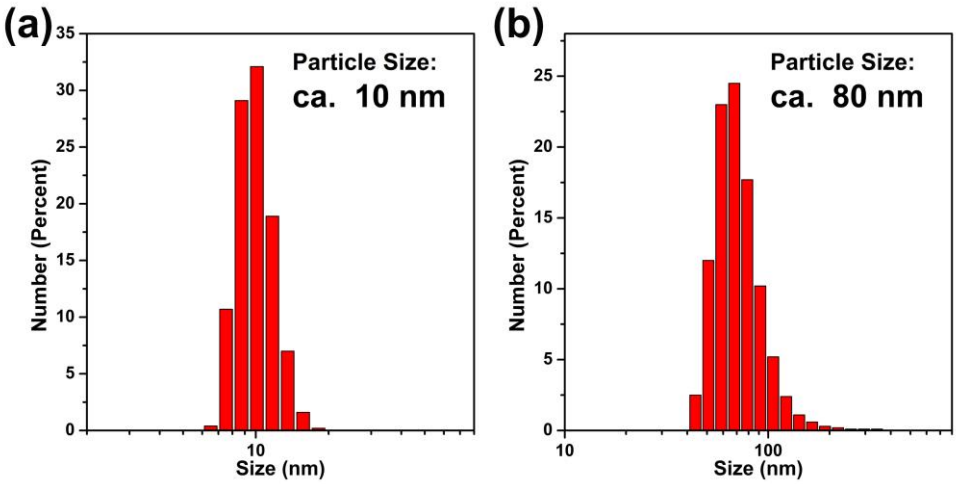

Figure S9. Dynamic light scattering characterization of Beta-∞-180-i precursors prepared with (a) and without (b) addition of L-lysine after microwave irradiation.

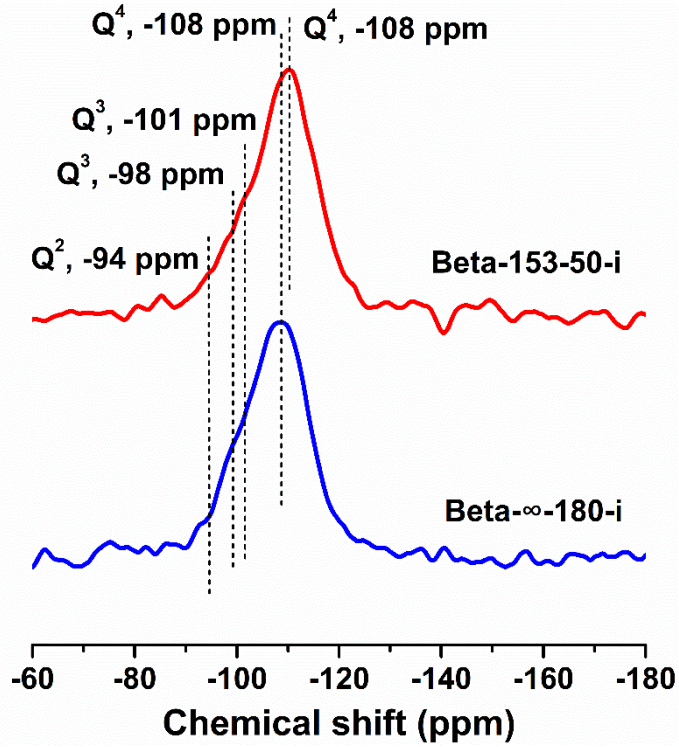

Figure S10. ^{29}Si solid-state MAS NMR spectra of Beta-153-50-i and Beta-∞-180-i precursors treated after microwave irradiation.

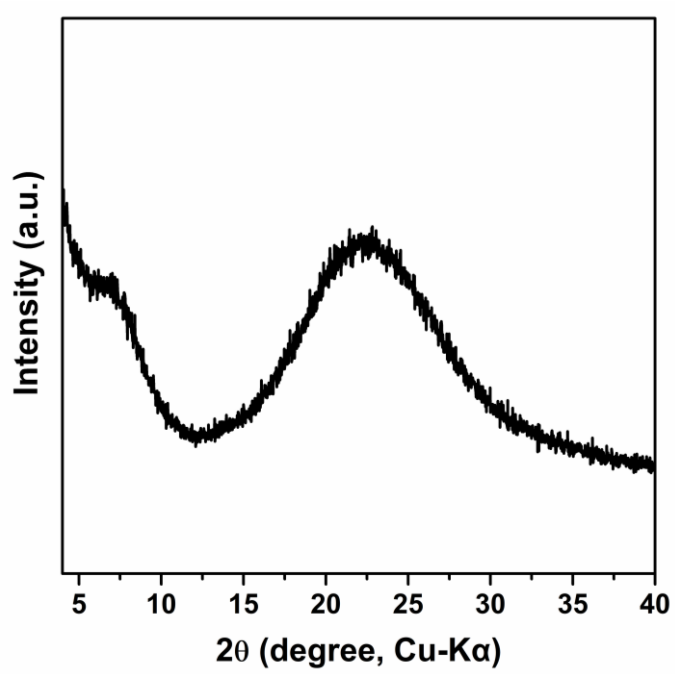

Figure S11. PXRD pattern of Al-free sample obtained via a two-step microwave-assisted crystallization.

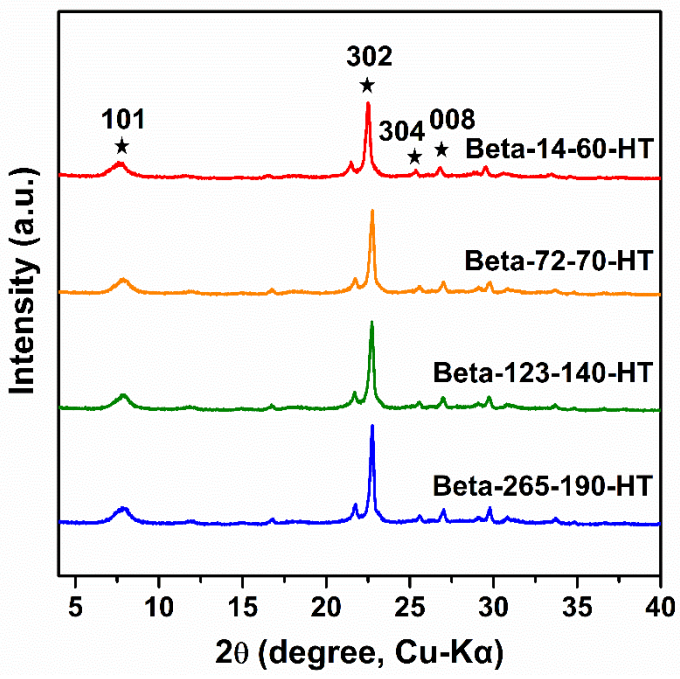

Figure S12. PXRD patterns of Beta zeolites with varied Si/Al ratios obtained via two-step hydrothermal crystallization.

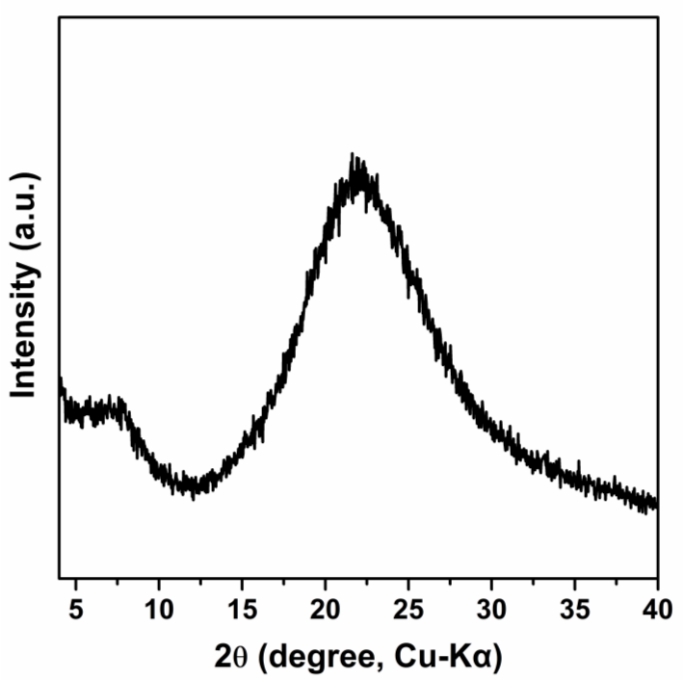

Figure S13. PXRD pattern of Al-free sample obtained via a two-step hydrothermal crystallization.

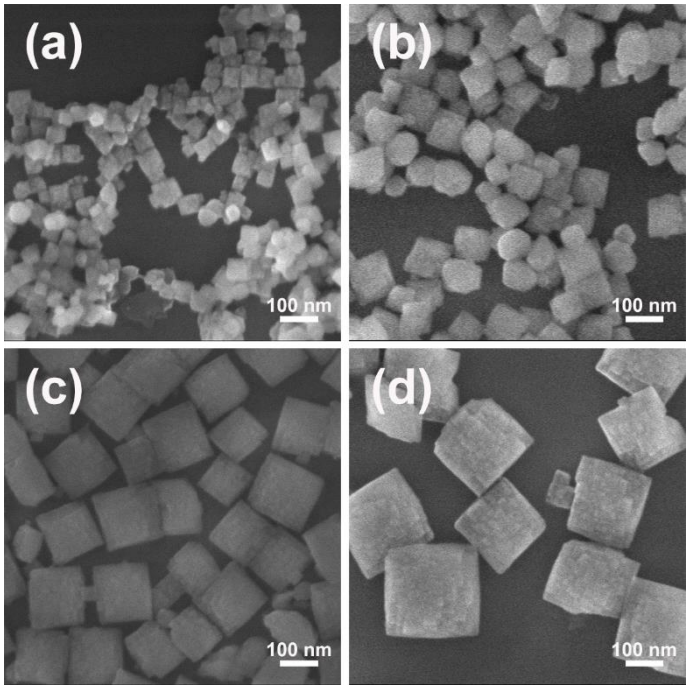

Figure S14. SEM images of Beta zeolites with varied Si/Al ratios obtained via two-step hydrothermal crystallization: (a) Beta-14-60-HT, (b) Beta-72-70-HT, (c) Beta-123-140-HT, (d) Beta-265-190-HT.

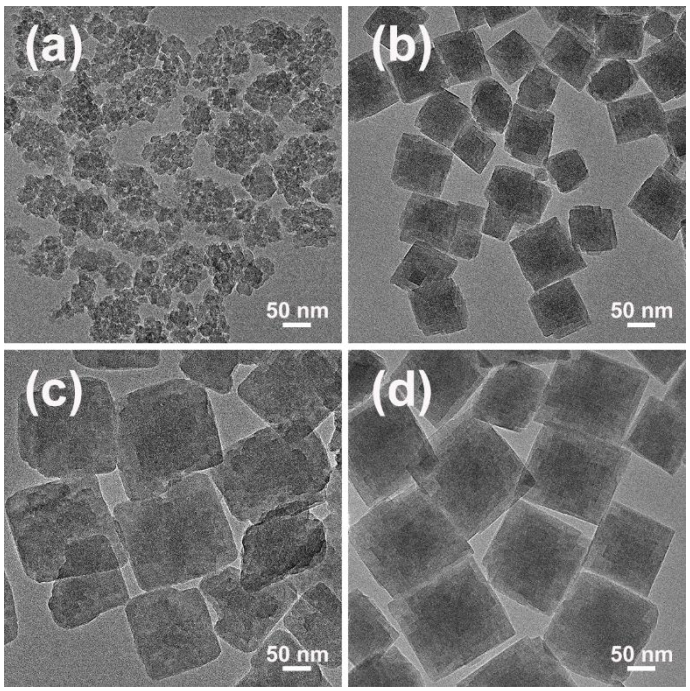

Figure S15. TEM images of Beta zeolites with varied Si/Al ratios obtained via two-step hydrothermal crystallization: (a) Beta-14-60-HT, (b) Beta-72-70-HT, (c) Beta-123-140-HT, (d) Beta-265-190-HT.

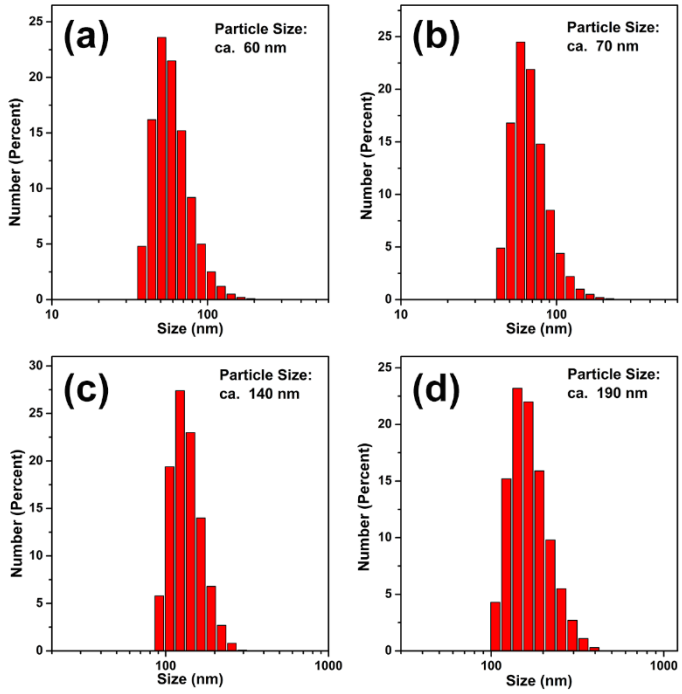

Figure S16. Dynamic light scattering characterization of Beta zeolites with varied Si/Al ratios obtained via two-step hydrothermal crystallization: (a) Beta-14-60-HT, (b) Beta-72-70-HT, (c) Beta-123-140-HT, (d) Beta-265-190-HT.

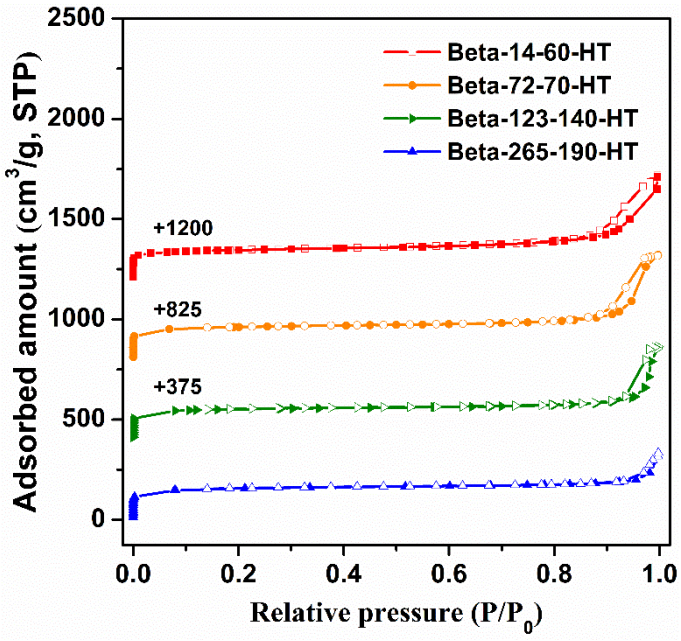

Figure S17. N_2 adsorption/desorption isotherms of Beta zeolites with varied Si/Al ratios obtained via two-step hydrothermal crystallization.

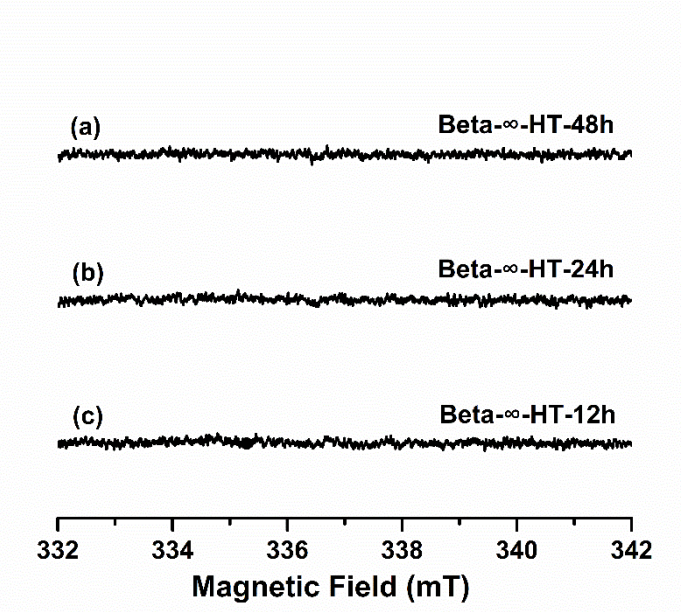

Figure S18. EPR spectra of the initial reaction mixture upon low-temperature hydrothermal for 12–48 h.

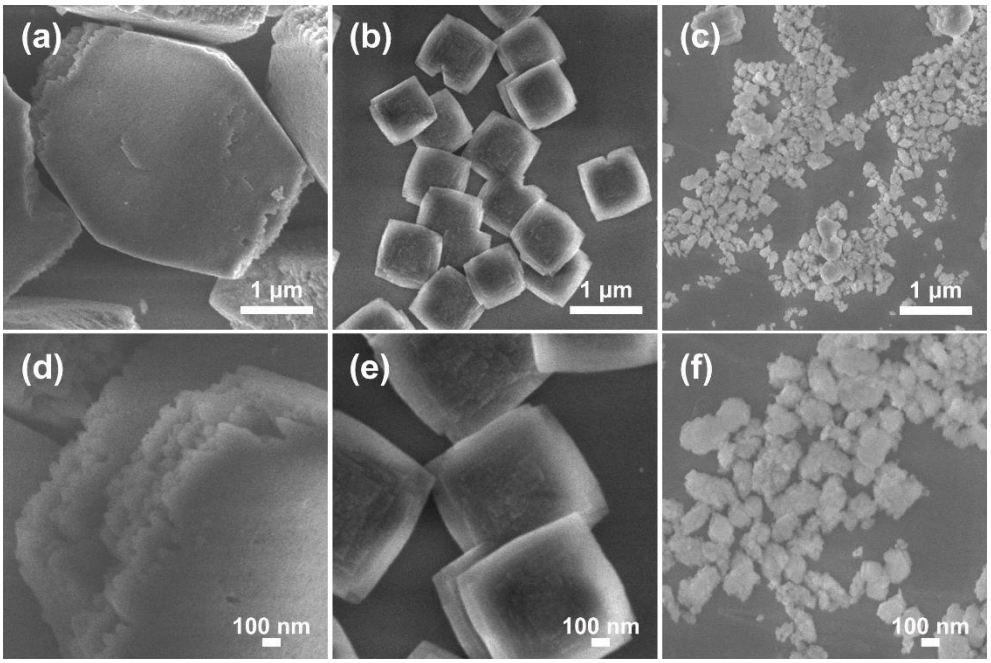

Figure S19. (a, b, c) Low-magnification scanning electron microscopy (SEM) images, (d, e, f) high-magnification SEM images of pure-silica Beta zeolites synthesized using different methods: (a, d) Beta-∞-HF, (b, e) Beta-∞-SAC, (c, f) Beta-∞-DA.

Table S1. Molar compositions of the initial mixtures and crystallization conditions of Beta zeolites.

Sample	Molar composition				Crystallization conditions				
					Step I			Step II HT	
	SiO_2	TEAOH	L-lysine	HF	Method	T_1 (°C)	t_1 (h)	T_2 (°C)	t_2 (h)
Beta-9-25-MW	1	0.55	0.2	/	MW[a]	80	4	140	6
Beta-15-28-MW	1	0.55	0.2	/	MW	80	4	140	6
Beta-77-30-MW	1	0.55	0.2	/	MW	80	4	140	6
Beta-153-50-MW	1	0.55	0.2	/	MW	100	4	140	6
Beta-338-100-MW	1	0.55	0.2	/	MW	100	4	140	10
Beta-∞-180-MW	1	0.55	0.2	/	MW	100	4	160	120
Beta-153-50-i	1	0.55	0.2	/	MW	100	4	/	/
Beta-∞-180-i	1	0.55	0.2	/	MW	100	4	/	/
Beta-14-60-HT	1	0.55	0.2	/	HT[b]	80	48	140	48
Beta-72-70-HT	1	0.55	0.2	/	HT	80	48	140	48
Beta-123-140-HT	1	0.55	0.2	/	HT	80	48	140	48
Beta-265-190-HT	1	0.55	0.2	/	HT	80	48	140	48
Beta-∞-SAC	1	0.42	/	/	SAC[c]	140	120	/	/
Beta-∞-HF	1	0.40	/	0.4	HT	150	168	/	/

[a] Microwave-assisted synthesis. [b] Hydrothermal treatment. [c] Steam-assisted conversion.

Table S2. Fast synthesis of Beta zeolites with different Si/Al ratios particles summered from references.

Si/Al ratios	Particle Size	Synthesis method	Crystallization condition	Ref.
15-50	70-100 nm	Microwave-assisted	80 °C/1.5 h-150 °C/4.5 h	4
12.5	400-500 nm	Microwave-assisted	170 °C, 4 h	5
7-11	500 nm	Interzeolite conversion	125 °C, 2 h	6
300	0.3 μm	Interzeolite conversion	190 °C, 3 h	7
10-33	20 nm	Steam-assisted	170-180 °C, 6-7 h	8
10.2	100 nm	Seed-induced	140 °C, 18.5 h	9
15	10 μm	High-temperature	200 °C, 2 h	10
50-∞	1 μm	Dry-gel conversion	160 °C, 8 h	11
45	500 nm	Sealed pipe reactor	210 °C, 10 min	12
20-160	60 nm	Steam-assisted	150 °C, 8 h	13

Table S3. Selected pure-silica Beta zeolites reported in the literature and their synthesis methods, Si/Al ratios, and particle size.

Si/Al ratios	Particle size	Synthesis method	Mineralizer	Assistant	Crystallization condition	Ref.
25-∞	0.3-0.4 μm	Hydrothermal	HF	Seed	120-180 ºC, 9 d	14
Infinite	0.3-0.4 μm	Hydrothermal	/	Seed	140 ºC, 4 d	15
Infinite	/	Hydrothermal	HF	/	135 ºC, 7 d	16
15-∞	60 nm	DGC[a]	NaOH	/	145 ºC, 5 d	17
Infinite	0.5 μm	DGC	NaOH	/	145 ºC, 5 d	18
130-510	0.2-0.6 μm	Hydrothermal	NaOH	SDA[b]	135 ºC, 1-4 d	19
Infinite	0.14 μm	Hydrothermal	NaOH	SDA[c]	100 ºC, 3-4 d	20
Infinite	30-70 nm	Inter. Trans.[d]	/	Seed	140 ºC, 2 d	21
Infinite	1 μm	Solvent-free	NH_4F	Seed	140 ºC, 5 d	22

[a] DGC: Dry gel conversion. [b] 4,4'-trimethylene-bis (N-benzyl-N-methylpiperidinium)-dihydroxide. [c] 4,4'-trimethylenebis (N-methyl, N-benzyl-piperidinium). [d] Interzeolite transformation.

Table S4. Porosities of pure-silica Beta zeolites synthesized by traditional synthesis methods.

Sample	S_{BET}[a] ($m^2\ g^{-1}$)	S_{micro}[b] ($m^2\ g^{-1}$)	S_{ext}[b] ($m^2\ g^{-1}$)	V_{total}[c] ($cm^3\ g^{-1}$)	V_{meso}[d] ($cm^3\ g^{-1}$)	V_{micro}[b] ($cm^3\ g^{-1}$)
Beta-∞-HF	403	337	66	0.31	0.14	0.17
Beta-∞-SAC	373	268	105	0.40	0.26	0.14
Beta-∞-DA	440	290	150	0.60	0.45	0.15

[a]S_{BET}: total surface area, calculated by the BET method. [b]S_{micro}: micropore surface area, S_{ext}: mesopore surface area, and V_{micro}: micropore volume, calculated by the t-plot method. [c]V_{total}: total pore volume. [d]V_{meso}: mesopore volume, $V_{meso} = V_{total} - V_{micro}$

Table S5. Intensities and assignments obtained from the deconvolution of the ^{29}Si MAS NMR for three pure-silica Beta zeolites.

Attribution	Chemical shift (ppm)	Area (%)			
		Beta-∞-180-MW	Beta-∞-HF	Beta-∞-SAC	Beta-∞-DA
Q^3	-101	4.2	5.3	1.6	6.2
Q^4	-105	6.0	9.3	2.2	8.8
	-111/-112	62.5	59.2	67.7	59.4
	-115	27.3	26.2	28.5	25.6

Table S6. Langmuir, Sips equation correlation parameters and fitting results for different Beta zeolites.

	Langmuir Model			Sips Model			
Toluene	q_m	b	R^2	q_m	b	n	R^2
Beta-∞-180-MW	15240	0.0067	0.94	13790	0.0073	1.02	0.95
Beta-∞-HF	5001	0.019	0.75	10670	0.0079	1.69	0.78
Beta-∞-SAC	60.1	18.4	0.93	54.3	248.5	0.63	0.94
Beta-∞-DA	48.3	12.4	0.91	78.1	1.49	1.49	0.92
	Langmuir Model			Sips Model			
Water	q_m	b	R^2	q_m	b	n	R^2
Beta-∞-180-MW	15610	0.006	0.99	8673	0.011	0.94	0.99
Beta-∞-HF	116.5	0.102	0.99	2408	0.0044	1.10	0.99
Beta-∞-SAC	2865	0.075	0.99	6883	0.029	1.08	0.99
Beta-∞-DA	16750	0.014	0.98	14220	0.015	0.87	0.99

1. E. B. Lami, F. Fajula, D. Anglerot and T. Des Courieres, *Microporous Materials*, 1993, **1**, 237-245.
2. H. Yi, H. Deng, X. Tang, Q. Yu, X. Zhou and H. Liu, *J. Hazard. Mate.*, 2012, **203**, 111–117.
3. R. T. Yang, *John Wiley & Sons*, 2003.
4. Y. Hu, C. Liu, Y. Zhang, N. Ren and Y. Tang, *Micropor. Mesopor. Mat.*, 2009, **119**, 306–314.
5. H.-S. You, H. Jin, Y.-H. Mo and S.-E. Park, *Mater. Lett.*, 2013, **108**, 106–109.
6. K. Honda, A. Yashiki, M. Itakura, Y. Ide, M. Sadakane and T. Sano, *Micropor. Mesopor. Mat.*, 2011, **142**, 161–167.
7. B. Wang, L. Ren, J. Zhang, R. Peng, S. Jin, Y. Guan, H. Xu and P. Wu, *Micropor. Mesopor. Mat.*, 2021, **314**, 110894.
8. K. Möller, B. Yilmaz, R. M. Jacubinas, U. Müller and T. Bein, *J. Am. Chem. Soc.*, 2011, **133**, 5284–5295.
9. B. Xie, H. Zhang, C. Yang, S. Liu, L. Ren, L. Zhang, X. Meng, B. Yilmaz, U. Müller and F.-S. Xiao, *Chem. Commun.*, 2011, **47**, 3945–3947.
10. C. Bian, C. Zhang, S. Pan, F. Chen, W. Zhang, X. Meng, S. Maurer, D. Dai, A.-N. Parvulescu and U. Müller, *J. Mater. Chem. A*, 2017, **5**, 2613–2618.
11. X. Zhao, L. Wang, P. Guo, N. Yan, T. Sun, S. Lin, X. Guo, P. Tian and Z. Liu, *Catal. Sci. Technol.*, 2018, **8**, 2966–2974.
12. J. Zhu, Z. Liu, S. Sukenaga, M. Ando, H. Shibata, T. Okubo and T. Wakihara, *Micropor. Mesopor. Mat.*, 2018, **268**, 1–8.
13. T.-L. Cui, J.-Y. He, M. Hu, C.-S. Liu and M. Du, *Micropor. Mesopor. Mat.*, 2020, **309**, 110448.
14. Y. Kalvachev, M. Jaber, V. Mavrodinova, L. Dimitrov, D. Nihtianova and V. Valtchev, *Micropor. Mesopor. Mat.*, 2013, **177**, 127–134.
15. D. Luo, Q. Wang, D. Fan, M. Yang, B. Fan, K. Cao, S. Xu, P. Tian and Z. Liu, *Micropor. Mesopor. Mat.*, 2022, **329**, 111557.
16. M. Van den Bergh, A. Krajnc, S. Voorspoels, S. R. Tavares, S. Mullens, I. Beurroies, G. Maurin, G. Mali and D. E. De Vos, *Angew. Chem. Int. Ed.*, 2020, **59**, 14086–14090.
17. P. H. P. Rao, K. Ueyama and M. Matsukata, *Appl. Catal. A*, 1998, **166**, 97–103.
18. V. Vattipalli, A. M. Paracha, W. Hu, H. Chen and W. Fan, , *Angew. Chem. Int. Ed.*, 2018, **57**, 3607–3611.

19. M. Bregolato, V. Bolis, C. Busco, P. Ugliengo, S. Bordiga, F. Cavani, N. Ballarini, L. Maselli, S. Passeri and I. Rossetti, *J. Catal*., 2007, **245**, 285–300.
20. O. Larlus, S. Mintova, S. T. Wilson, R. R. Willis, H. Abrevaya and T. Bein, *Micropor. Mesopor. Mat.*, 2011, **142**, 17–25.
21. Z. Zhu, H. Xu, J. Jiang, H. Wu and P. Wu, *ACS Appl. Mater. Inter.*, 2017, **9**, 27273–27283.
22. Q. Wu, X. Liu, L. Zhu, L. Ding, P. Gao, X. Wang, S. Pan, C. Bian, X. Meng and J. Xu, *J. Am. Chem. Soc.*, 2015, **137**, 1052–1055.